

Behaviour of Di-Transition-Metal Nitride $\text{Ti}_{1-x}\text{Zr}_x\text{N}$ Alloy at High Pressure

T. CHIHI, S. BOUCETTA* AND D. MAOUCHE

Laboratoire d'Elaboration de Nouveaux Matériaux et leurs Caractérisations (ENMC)

Departement de Physique, Université Ferhat Abbas, Setif 19000, Algeria

(Received May 21, 2009; in final form October 3, 2009)

By means of density-functional theory with the generalized gradient approximation and using the virtual-crystal approximation, we report first-principles calculation results on the structural and elastic properties of $\text{Ti}_{1-x}\text{Zr}_x\text{N}$ alloy. In order to gain some further information on the mechanical properties of $\text{Ti}_{0.5}\text{Zr}_{0.5}\text{N}$ compound, we also calculated the Young modulus, Poisson ratio, and anisotropy factor. The variation of calculated unit cell parameter for $\text{Ti}_{1-x}\text{Zr}_x\text{N}$ structure increases with Zr content x . A linear dependence of the elastic constants and the bulk modulus over a range of composition x is found. All the C_{ij} of $\text{Ti}_{0.5}\text{Zr}_{0.5}\text{N}$ increase linearly with increasing pressure. The same behaviour is observed for the other compounds with Zr compositions x .

PACS numbers: 81.40.Jj, 63.20.dk, 62.50.-p

1. Introduction

The aim of this article is to examine the structural, elastic, and mechanical properties of cubic rock-salt $\text{Ti}_{1-x}\text{Zr}_x\text{N}$ alloy, with emphasis on their dependence on hydrostatic pressure. The transition-metal nitrides have attracted considerable attention during the past three decades due to their interesting combination of mechanical, electrical, and chemical properties. This has led to their wide application as hard coatings and thin films for electronic devices [1]. In addition to their stability at high temperatures, these compounds are extremely hard, finding industrial use in cutting tools and wear-resistant parts. Their hardness is retained to very high temperatures, and they have low chemical reactivity. Transition-metal nitrides and carbides in the rock-salt (*B1*) structure are widely used for cutting tools and generators due to their high hardness, high melting points, and oxidation resistance [2]. Mixed-metal carbides and nitrides have been examined for their melting point and hot hardness behaviour as well. It has been demonstrated that intermediate compositions of the ternary system formed with *3d* metals (TiN, TiC), *4d* (ZrN, ZrC) are harder than the corresponding binary compounds [3]. There have been several earlier first-principles studies into properties of these materials: Papaconstantopoulos et al. [4] studied group V and VI transition-metal mononitrides, focusing on superconducting properties. Stampfl et al. [5] investigated the electronic structure and physical properties of early transition-metal mononitrides. Dayong Cheng et al. [6] studied the elastic properties of ZrC and ZrN. Nagao et al. [7] studied group IVB transition-metal

mononitrides, focusing on anisotropic elasticity. Hoerling et al. [8] investigated thermal stability, microstructure, and mechanical properties of $\text{Ti}_{1-x}\text{Zr}_x\text{N}$ thin films. The question is then if it is possible to make artificial materials that match or exceed the hardness of the hardest known materials-group IV nitrides (TiN and ZrN).

The group IV nitrides (TiN and ZrN) crystallize only in the cubic NaCl structure. The NaCl (*B1*) structure is common to both the mononitrides and the monocarbides. The transition-metal mononitrides have face centered cubic structures, with space group *Fm-3m*. TiN and ZrN display many of the properties common to the other transition metal nitrides: hard ceramic material, and a large range of homogeneity. In view of these properties it seems worthwhile to model the mechanical behaviour at the atomistic level for the di-transition-metal nitrides: $\text{Ti}_{1-x}\text{Zr}_x\text{N}$.

In this work, we investigate the effect of substituting the Ti atoms in TiN binary alloy by zirconium atoms, i.e. the cubic $\text{Ti}_{1-x}\text{Zr}_x\text{N}$ alloy, on the elastic properties in this system.

This article is organized as follows: The computational method is described in Sect. 2. In Sect. 3, the results of the calculations are presented and compared with available experimental and theoretical data. Conclusion is given in Sect. 4.

2. Computational method

The use of computer simulation techniques is becoming more important in the understanding of the physical properties of materials. Our first-principles calculations are performed with the plane-wave pseudopotential (PWPP) method implemented by the CASTEP (abbreviation of Cambridge Serial Total Energy Package) sim-

* corresponding author; e-mail: boucetta_said02@yahoo.fr

ulation program [9]. This is based on the density functional theory (DFT) [10, 11] which is, in principle an exact theory of the ground state. The generalized gradient approximation (GGA), proposed by Perdew and Wang, known as PW91 [12], is made for electronic exchange–correlation potential energy. Coulomb potential energy caused by electron–ion interaction is described using ultrasoft scheme [13], in which the orbitals of Ti ($3d^24s^2$), Zr ($4d^25s^2$), and N ($2s^22p^3$) are treated as valence electrons. By the norm-conservation condition, the pseudo-wave function related to pseudopotential matches the plane-wave function expanded with Kohn–Sham formation beyond a cut-off energy. Using high cut-off (660 eV) energy at the price of spending long computational time can make accurate results. The cut-off energy for the plane-wave expansion is 380 eV and the Brillouin zone sampling was carried out using the $8 \times 8 \times 8$ set of the Monkhorst–Pack mesh [14]. Atomic positions are relaxed and optimized with a density mixing scheme [15] using

the conjugate gradient (CG) method [16] for eigenvalues minimization.

The equilibrium lattice parameter is computed from the structural optimization, using the Broyden–Fletcher–Goldfarb–Shanno (BFGS) minimization technique.

3. Results and discussion

3.1. Structural properties

For the treatment of the disordered ternary alloy, we used the virtual crystal approximation (VCA) [17], in which the alloy pseudopotentials are constructed within a first-principles VCA scheme. Elemental ionic pseudopotentials of TiN and ZrN are combined to construct the virtual pseudopotential of $\text{Ti}_{1-x}\text{Zr}_x\text{N}$:

$$V_{\text{VCA}} = xV_{\text{ZrN}} + (1 - x)V_{\text{TiN}}. \quad (1)$$

TABLE I

Lattice constant, bulk modulus and elastic constants for cubic $\text{Ti}_{1-x}\text{Zr}_x\text{N}$ in comparison with experimental and theoretical data.

| Zirconium fraction | 0 | 0.25 | 0.50 | 0.75 | 1 |
|--------------------|---|--------------------|--------------------|--------------------|---|
| a_0 [Å] | 4.271 | 4.385 | 4.478 | 4.553 | 4.615 |
| experimental | 4.24 ^a , 4.242 ^b , 4.235 ^c | 4.430 ^l | 4.532 ^l | 4.51 ^k | 4.537 ^b , 4.61 ^c , 4.574 ^f |
| calculated | 4.246 ^d , 4.26 ^e | 4.325 ^k | 4.422 ^k | 4.493 ^k | 4.57 ^e , 4.564 ^g , 4.58 ^k , 4.593 ^d |
| B [GPa] | 272.5 | 273.14 | 268.47 | 264.79 | 257.80 |
| experimental | 288 ^h | | | | 215 ⁱ |
| calculated | 286.6 ^d , 286.0 ^e , 303 ^k | 292.5 ^k | 284 ^k | 277 ^k | 257.9 ^d , 272 ^k , 285 ⁱ , 264 ^e |
| C_{11} [GPa] | 614.288 | 625.798 | 623.813 | 618.639 | 606.010 |
| experimental | 625 ^j | | | | 471 ⁱ |
| calculated | 585 ^d | | | | 537 ^d , 611 ⁱ |
| C_{12} [GPa] | 101.60 | 96.80 | 90.80 | 87.87 | 83.69 |
| experimental | 165 ^j | | | | 88 ⁱ |
| calculated | 585 ^d | | | | 118 ^d , 117 ⁱ |
| C_{44} [GPa] | 178.38 | 163.88 | 153.87 | 144.83 | 139.07 |
| experimental | 163 ^j | | | | 138 ⁱ |
| calculated | 165 ^d | | | | 120 ^d , 129 ⁱ |

^aRef. [18], ^bRef. [19], ^cRef. [20], ^dRef. [7], ^eRef. [5], ^fRef. [21], ^gRef. [6], ^hRef. [22], ⁱRef. [23], ^jRef. [24], ^kRef. [8], ^lRef. [29]

The results for lattice parameter a_0 are reported for different composition rates x in Table I and compared with experiment [18–29, 17] and previous theoretical calculations [5–7]. Our calculated value for lattice parameter a_0 of TiN is in good agreement with the experimental data calculated by Helmersson et al. [18] and it is little higher than theoretical values [5, 7] ones. We have obtained the same value for a_0 of ZrN as experimental [20] one, but it is higher than the calculated values [5, 7]. Our

calculated lattice parameters of $\text{Ti}_{1-x}\text{Zr}_x\text{N}$ ($x = 0.25, 0.50, \text{ and } 0.75$) are well with the experimental data calculated by Uglov et al. [29].

In Fig. 1, we show the variation of the lattice parameter a_0 vs. zirconium fraction x . An analytical relation for the compositional dependence of $\text{Ti}_{1-x}\text{Zr}_x\text{N}$ lattice parameter is given by a quadratic fit

$$a(x) = 4.27 + 0.48x - 0.14x^2. \quad (2)$$

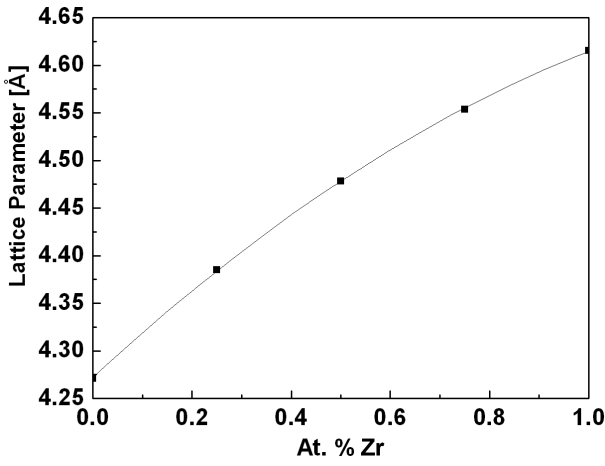


Fig. 1. Related lattice parameter of $Ti_{1-x}Zr_xN$ as a function of composition (x).

3.2. Elastic constants

The elastic constants of solids provide a link between the mechanical and dynamical behaviours of crystals, and give important information concerning the nature of the forces operating in solids. In particular, they provide information on the stability and stiffness of materials. It is very well known that the first-order and second-order derivatives of the potential give forces and elastic constants. Therefore, it is an important issue to check the accuracy of the calculations for forces and elastic constants. The effect of pressure on the elastic constants is essential, i.e., for understanding interatomic interactions, mechanical stability, and phase transition mechanisms. According to Hooke's law [25], the stress σ and strain ε for small deformations to a crystal are linearly related by

$$\sigma_{ij} = C_{ijkl}\varepsilon_{kl} \quad (i, j, k, l = 1, 2, 3), \quad (3)$$

where the fourth-rank tensor C_{ijkl} is the elastic constant tensor. Thus, the elastic constants can be determined directly from the computation of the stress generated by small strains [26]. The cubic crystal has three independent elastic constants, C_{11} , C_{12} and C_{44} .

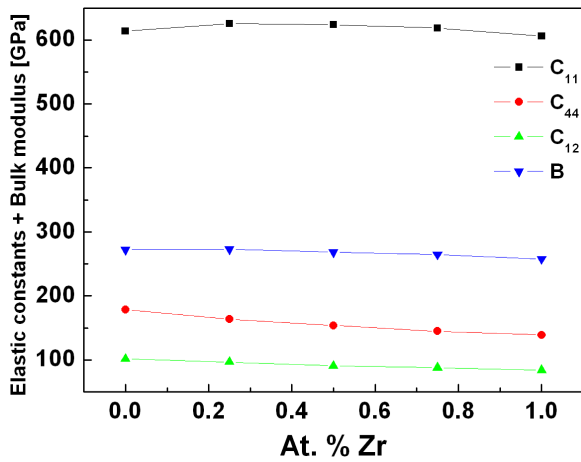


Fig. 2. Compositional dependence of the elastic constants and the bulk modulus.

C_{44} of ZrN agrees well with the experimental [23] value. In the case of TiN, it can be noted from Table I that our calculated value of C_{11} is little lower than the corresponding experimental [24] one, but the C_{11} of ZrN calculated value is higher than the experimental data [23]. However, simulated values for C_{12} in this work for both ZrN and TiN are lower than the experimental values [23, 24], respectively.

The obtained results for the composition dependence of the elastic constants are depicted in Fig. 2. The curves of elastic constants show a linear increase from TiN to ZrN. Our calculated bulk modulus for TiN is smaller but for ZrN it is higher than the experimental values [22, 23], respectively. It can be seen that the compositional dependence of the bulk modulus is linear (Fig. 2).

3.3. Pressure effect on elastic properties

We have calculated the three elastic constants $C_{11}(x)$, $C_{12}(x)$ and $C_{44}(x)$ for $x = 0.5$ from the stress-strain up to 50 GPa, in order to study the elastic stability. As it is shown in Fig. 3, we remark that all C_{ij} increase linearly

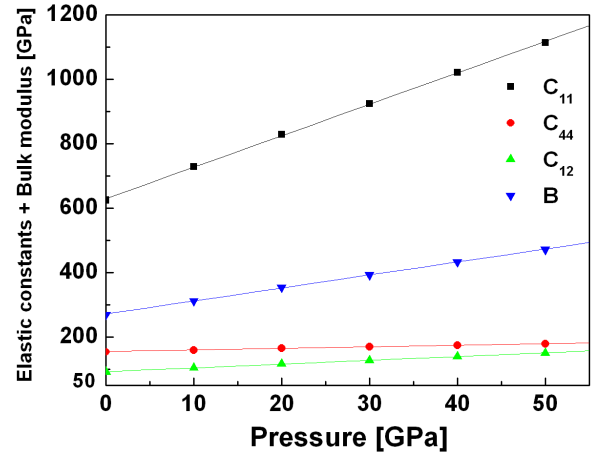


Fig. 3. Elastic constants C_{11} , C_{12} , and C_{44} vs. pressure of $Ti_{0.5}Zr_{0.5}N$. ■, our data and —, linear fit.

with increasing pressure. These elastic constants satisfy the generalized elastic stability criteria for cubic crystals under hydrostatic pressure, $C_{11} + C_{12} > 0$, $C_{44} > 0$ and $C_{11} - C_{12} > 0$. The values of the bulk modulus B increase with pressure and reach 471 GPa at pressure of 50 GPa. At 40 GPa, the bulk modulus of $Ti_{0.5}Zr_{0.5}N$ reaches the zero-pressure value of the bulk modulus of the diamond [27]. The elastic anisotropy at high pressure is important for understanding the evolution of bonding in the system. The Zener anisotropy factor A , Poisson ratio ν and Young modulus Y , which are the most interesting elastic properties for applications, are often measured for polycrystalline materials when investigating their hardness. $A = 2C_{44}/(C_{11} - C_{12})$ measure the anisotropy of the elasticity for cubic crystal. The quantities ν and Y are calculated in terms of the computed data using the following relations [28]:

$$\nu = \frac{1}{2} \frac{B - \frac{2}{3}G}{B + \frac{1}{3}G}, \quad (4)$$

$$Y = \frac{9GB}{G + B}. \quad (5)$$

In Fig. 4, we plot the pressure dependence of A for cubic $\text{Ti}_{0.5}\text{Zr}_{0.5}\text{N}$ compound. The anisotropy factor shows a gradual decrease with increasing pressure. As a result, we observe that $G_{\{110\}} > G_{\{100\}}$, indicating that it is easier to shear on the $\{100\}$ plane along the $[010]$ direction rather than on the $\{110\}$ plane along the $[1-10]$ direction. The calculated Poisson ratio (ν) and Young modulus (Y) for cubic $\text{Ti}_{0.5}\text{Zr}_{0.5}\text{N}$ compound are given in Table II. The values of the moduli B and G suggest a large hardness in this material with comparison of the bulk and Young moduli of the super hard material cubic boron nitride (BN).

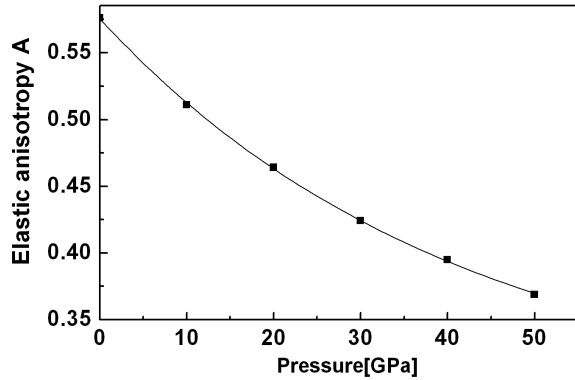


Fig. 4. Pressure dependence of the elastic anisotropy A for $\text{Ti}_{0.5}\text{Zr}_{0.5}\text{N}$.

TABLE II

The calculated Poisson ratio (ν) and Young modulus (Y).

| Material | Reference | ν | Y [GPa] |
|--|---------------|-------------------|-------------------------------------|
| $\text{Ti}_{0.5}\text{Zr}_{0.5}\text{N}$ | present (GGA) | 0.215 | 601.538 |
| | other | 0.22 ^l | 477 ^k , 455 ^l |
| TiN | present (GGA) | 0.142 | 585.45 |
| | other | 0.25 ^l | 510 ^k , 470 ^l |
| ZrN | present (GGA) | 0.1213 | 585.70 |
| | other | 0.19 ^l | 457 ^k , 460 ^l |

^kRef. [8], ^lRef. [29]

4. Conclusion

In this paper, we have performed *ab initio* calculations of structural and elastic properties for cubic $\text{Ti}_{1-x}\text{Zr}_x\text{N}$ alloy, based on DFT, within the GGA, using the plane-wave pseudopotential approach. The results are summarized as follows:

- The calculated lattice parameter has a quadratic form with zirconium composition x .
- The elastic constants have a linear form with zirconium composition x .
- The bulk modulus and elastic stiffness coefficients of $\text{Ti}_{0.5}\text{Zr}_{0.5}\text{N}$ increase with increasing pressure in the range up to 50 GPa.
- The computed results for the bulk and Young moduli suggest a large hardness in this material.

We hope that this work will inspire future experimental research on these alloys, di-transition-metal nitrides.

Acknowledgments

We thank Professor L. Louail for providing the CASTEP used in performing this calculation. This work is supported by the ENMC laboratory, University of Setif.

References

- [1] H.O. Pierson, *Handbook of Refractory Carbides and Nitrides*, Noyes Publ., New Jersey 1996.
- [2] L.E. Toth, *transition-metal Carbides and Nitrides*, Academic Press, New York 1971.
- [3] H. Holleck, *J. Vac. Sci. Technol. A* **4**, 2621 (1992).
- [4] D.A. Papaconstantopoulos, W.E. Pickett, B.M. Klein, L.L. Boyer, *Phys. Rev. B* **31**, 752 (1985).
- [5] C. Stampfl, W. Mannstadt, R. Asahi, A.J. Freeman, *Phys. Rev. B* **63**, 155106 (2001).
- [6] D. Cheng, S. Wang, H. Ye, *J. Alloys Comp.* **377**, 221 (2004).
- [7] S. Nagao, K. Nordlund, R. Nowak, *Phys. Rev. B* **73**, 144113 (2006).
- [8] A. Hoerling, J. Sjöln, H. Willmann, T. Larsson, M. Odén, L. Hultman, *Thin Solid Films* **516**, 6421 (2008).
- [9] M.D. Segall, P.J.D. Lindan, M.J. Probert, C.J. Pickard, P.J. Haspin, S.J. Clark, M.C. Payne, *J. Phys., Condens. Matter* **14**, 2717 (2002).
- [10] P. Hohenberg, W. Kohn, *Phys. Rev. B* **136**, 864 (1964).
- [11] W. Kohn, L.J. Sham, *Phys. Rev. A* **140**, 113 (1965).
- [12] J.P. Perdew, J.A. Chevary, S.H. Vosko, K.A. Jackson, M.R. Pederson, D.J. Singh, C. Fiolhais, *Phys. Rev. B* **46**, 6671 (1992).
- [13] J. Furthmüller, P. Käckell, F. Bechstedt, *Phys. Rev. B* **61**, 4576 (2000).
- [14] H.J. Monkhorst, J.D. Pack, *Phys. Rev. B* **13**, 5188 (1976).
- [15] J.S. Lin, A. Qteish, M.C. Payne, V. Heine, *Phys. Rev. B* **47**, 4174 (1993).
- [16] A.M. Rappe, K.M. Rabe, E. Kaxiras, J.K. Joannopoulos, *Phys. Rev. B* **41**, 1227 (1990).
- [17] L. Nordheim, *Ann. Phys. (Leipzig)*, 9607 (1931).

- [18] U. Helmersson, B.O. Johansson, J.E. Sundgren, *J. Vac. Sci. Technol. A* **3**, 308 (1985).
- [19] Structure Reports, Ed. W.B. Pearson, *TiN*, Vol. 11, International Union of Crystallography, Oosthock, Scheltema, and Holkema, Utrecht, 1993, p. 170.
- [20] R.W.G. Wyckoff, *Crystal Structures*, Vol. 1, 2nd ed., Wiley, New York 1963, p. 86.
- [21] J. Pfluger, J. Fink, W. Weber, K.P. Bohnen, *Phys. Rev. B* **31**, 1244 (1985).
- [22] V.P. Zhukov, V.A. Gubanov, O. Jepsen, N.E. Christensen, O.K. Andersen, *J. Phys. Chem. Solids* **49**, 841 (1988).
- [23] X.J. Chen, V.V. Struzhkin, Z.G. Wu, M. Somayazulu, J. Qian, S. Kung, A.N. Christensen, Y.S. Zhao, R.E. Cohen, H.K. Mao, R.J. Hemley, *Appl. Phys. Sci.* **102**, 3198 (2005).
- [24] J.O. Kim, J.D. Achenbach, P.B. Mirkarimi, M. Shinn, S.A. Barnett, *J. Appl. Phys.* **72**, 1805 (1992).
- [25] J.F. Nye, *Physical Properties of Crystals*, Clarendon, Oxford (UK) 1985 p. 329.
- [26] R.M. Wentzcovitch, N.L. Ross, G.D. Price, *Phys. Earth Planetary Interiors* **90**, 101 (1995).
- [27] F. Occelli, P. Loubeyre, R. Letoullec, *Nature Mater.* **2**, 151 (2003).
- [28] B. Mayer, H. Anton, E. Bott, M. Methfessel, J. Sticht, P.C. Schmidt, *Intermetallics* **11**, 23 (2003).
- [29] V.V. Uglov, V.M. Anishchik, S.V. Zlotski, G. Abadías, *Surf. Coat. Technol.* **200**, 6389 (2006).